Colloquium on Robotics, Unmanned Systems And Cybernetics 2014 (CRUSC 2014)
Nov. 20, 2014 at Universiti Malaysia Pahang, Pekan, Pahang, Malaysia

3D Image Construction Using Single LRF Hokuyo URG-04LX

Hendriyawan Achmad[1], Mohd Razali Daud[2]
[1,2] Faculty of Electrical & Electronics Engineering, University Malaysia Pahang, Pekan, 26600, Malaysia
(E-mail: hendriyawanachmad@gmail.com[1], mrazali@ump.edu.my[2])

Abstract – Nowadays researchers who focus on robotic vision technology are facing with greater challenges, where the 2D technology has many flaws in robot navigation. Using 3D technology, the robot is able to make a more detailed map navigation making it easier to carry out its mission. 3D image is obtained by using the method of fusion between the Hokuyo URG-04LX with 6-DOF IMU consists of acceleration sensor and gyro sensor. IMU sensor outputs are the angle, speed, and position in 3D. However, only the value of the angle is used in this work. To eliminate noise in the sensors output, two types of filters are used; the gaussian filter used on the output 2D LRF, while the complementary filter is used on the output of the IMU sensor. The proposed systems has successfully generated a valid 3D image according to the indoor testing that has been done.

Keywords – 3D image, Hokuyo URG-04LX, IMU sensor, filter.

1. Introduction

Mapping is the most important part of the mission of a mobile robot to recognize the surrounding environment[1], thus autonomous robots capable of moving and finding ways to avoid obstacles[2]. Mobile robot navigation technology is now increasingly sophisticated, with applying techniques of 2D and 3D navigation. Many studies on the implementation of 2D navigation for SLAM (simultaneous localization and mapping) to determine the current position of the robot in an area that has not been recognized previously[3]. However, current robotic missions more complex, not only to avoid obstacles and to find a way but also able to measure the dimensions of each part of the surrounding which is used in the context of path planning information.

There are many ways to get a 3D image[4] as the basis for the construction of a 3D map. Experiments that have been done in previous studies by using the 2D LRF and the 6-DOF IMU sensor[4][5][6][7]. IMU sensors provide 3-axis angle information are used to construct a 3D image and a 3-axis position information to build a 3D map.

This paper will discuss the methods of 3D image construction using the 2D LRF sensor Hokuyo URG-04lx and 6-DOF IMU sensor.

2. System Description

As mentioned before, in this paper uses two types of sensors are used; 2D LRF sensors Hokuyo URG-04LX to measure distances [8] and 6-DOF IMU sensor MPU6050 which is composed from 3-DOF acceleration sensor and 3-DOF gyro sensor to measure angles [9]. Figure 1 shows a picture from the 2 sensors.

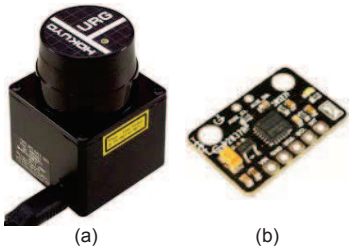

Fig. 1. (a) 2D LRF Hokuyo URG04LX (b) 6-DOF IMU sensor MPU6050

Since the 2D LRF sensor only capable of scanning in horizontal direction, a tilt mechanism with DC servo motor is used to enable the laser sensor scanning in vertical direction for $\pm 30^0$ range with 2^0 resolution. Changes in the angle will be measured by the IMU sensors, and used as input to establish 3D projection. Angle values are acquired from the fusion process between acceleration sensor and gyro sensor, at once as complementary filters that will be discussed in the next section. Arduino system is used for IMU sensor data acquisition and control DC servo tilt. Figure 2 shows a diagram of the system used in this work.

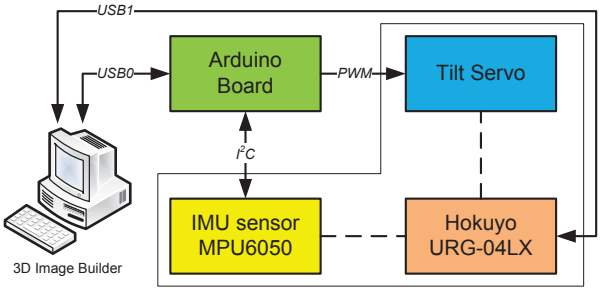

Fig. 2. Block diagram represention of control flow

ISBN 978-967-0691-42-8

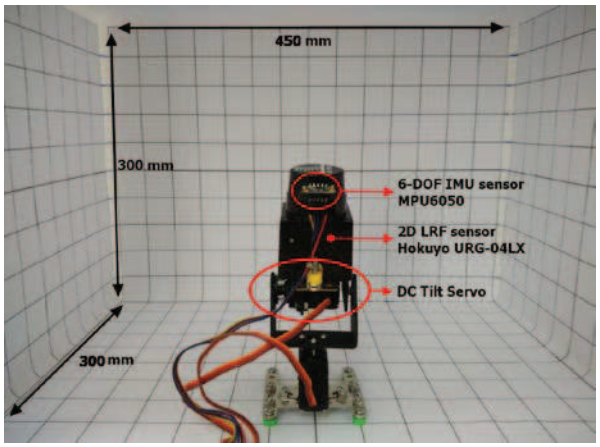

Fig. 3. Test Bed system for 3D space construction

On the other hand, Figure 3 shows the test bed used for the acquisition of 3D image data. In this work, Operational mode of 2D LRF sensor Hokuyo URG-04LX adjusted in accordance with the default, namely: horizontal scanning 240^0 with step 682 which gives the angular resolution 0.35^0 per step[10].

3. Geometry Invariant

By default, the number of valid data of Hokuyo URG-04LX are 682, start from 44^{th} data to 725^{th} data[10]. 2D projection of 682 data to form polar coordinates (r,θ), thus must be converted into 2D Cartesian coordinates (x_n,y_n) as shown by figure 4.

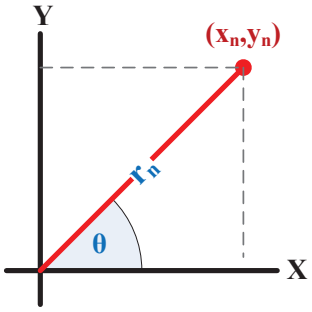

Fig. 4. Polar to cartesian projection

With the azimuth angle (θ) = step-n * 0.35° respect to X axis. Equation (1) and (2) show convertion steps from polar into cartesian.

$$x_n = r_n * \cos(\theta) \quad (1)$$

$$y_n = r_n * \sin(\theta) \quad (2)$$

Thus obtained 2 matrix which are shown by equation (3) and (4).

$$X = [x_0, x_1, x_2, \dots, x_{681}] \quad (3)$$

$$Y = [y_0, y_1, y_2, \dots, y_{681}] \quad (4)$$

To construct a 3D image in addition to the X axis and Y axis, Z axis is needed. To obtain the value of Z, scanning depth is required for each measurement angle in the range ± 30^0. Figure 5 shows the spherical polar coordinates are used for 3D projection..

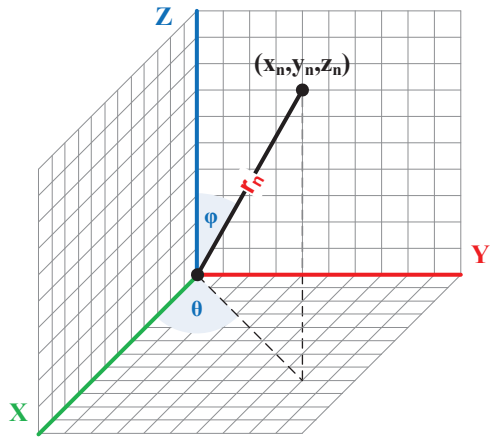

Fig. 5. Polar Spherical to 3D cartesian projection

Inclination angle (φ) obtained from IMU sensor and azimuth angle (θ) = step-n * 0.35°. Equation (5-7) show convertion steps from polar spherical into cartesian.

$$x_n = r_n * \cos(\theta) * \sin(\varphi) \quad (5)$$

$$y_n = r_n * \sin(\theta) * \sin(\varphi) \quad (6)$$

$$z_n = r_n * \sin(\theta) * \cos(\varphi) \quad (7)$$

Thus obtained 3 matrix shown by equation (8-10).

$$X = [x_0, x_1, x_2, \dots, x_{681}] \quad (8)$$

$$Y = [y_0, y_1, y_2, \dots, y_{681}] \quad (9)$$

$$Z = [z_0, z_1, z_2, \dots, z_{681}] \quad (10)$$

4. Data Filtering

LRF and IMU sensor outputs could be disrupted by noise that are influenced by the factors of the instrument from inside and outside. thus the filters are used to remove the noises. This paper uses two types of filters. Complementary filter applied to the 2 outputs of the IMU sensor (Acceleration and gyro), while 1D gaussian filter is applied to the 2D LRF sensor output.

4.1 Complementary Filter

This filter uses the input of acceleration sensor and gyro sensor to obtain clean output of noise with complementary method. Acceleration sensor measure all forces not only from the gravity vector alone, and easily distracted even with small force. Data from the acceleration sensor only reliable on the long term and the most appropriate filter is a low pass filter to remove noise on acceleration sensor. Gyro sensor measure angular velocity and less affected by external force, but the drift will always produce the result that can not go to zero when the system returns to its original position. Complementary filter utilizes the advantages from the both sensors. On the short term, we use the data from the gyroscope, because it is very precise and not susceptible to external forces. On the long term, we use the data from the accelerometer, as it does not drift. Figure 6 shows a basic diagram of complementary filter.

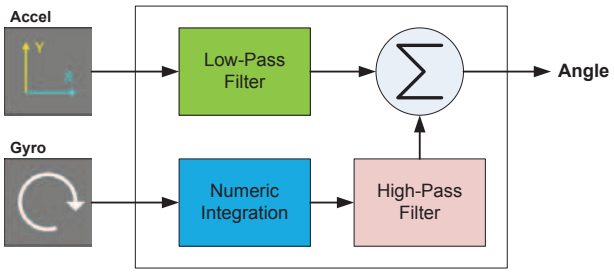

Fig. 6. Basic diagram of complementary filter

The diagram can be translated into mathematical equation as shown by equation 11.

$$angle = (0.98) * (angle + G_{out} * dt) + (0.02) * (A_{out}) \quad (11)$$

Time constant of the filter (τ) could be obtained based on equation 12.

$$\tau = \frac{\alpha.dt}{1-\alpha} \quad (12)$$

In this work, dt = 20mSec. Thus;

$$\tau = \frac{0.98*0.02}{0.02} = 0.98\ sec$$

This number as threshold value which is used to choose the between accelerometer and gyroscope function. If the value shorter than 0.98 sec, the gyroscope integration function is chosen and the noisy accelerations are filtered out. Otherwise, the accelerometer average function is given more weighting than the gyroscope.

4.2 Gaussian Filter

This filter is used to smooth the output of LRF sensor. In contrast to the 2D image smoothing method that uses a two-dimension gaussian filter, in this work used a one-dimensional gaussian filter. In mathematics, the 1D gaussian filter is written as shown by equation 13.

$$G(x) = \frac{1}{\sqrt{2\pi\sigma^2}} e^{-\left(\frac{x^2}{2\sigma^2}\right)} \quad (13)$$

Where σ is the standard deviation of the distribution. The distribution is assumed to have a mean (μ) of 0.

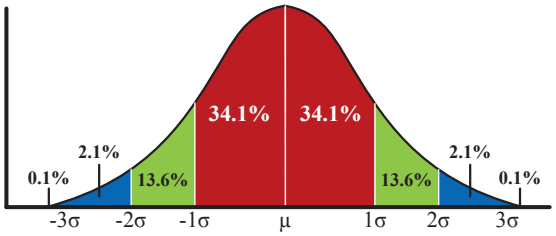

Fig. 7. Gaussian distribution function

The Standard deviation of the Gaussian function gives an important role in its action. The values located between +/- 1σ from the mean (red) account for 68% of the set, while +/- 2σ from the mean (red and green) account for 95%, and +/- 3σ from the mean (red, green and blue) account for 99.7%. Figure 7 shows gaussian distribution function.

5. Experimental Results

5.1 2D Polar to Cartesian

Output of LRF sensors Hokuyo URG-04LX in the form of a 2D polar coordinate converted into 2D Cartesian coordinate using equation 1 and 2. Figure 8 shows the experimental results of 2D data acquisition.

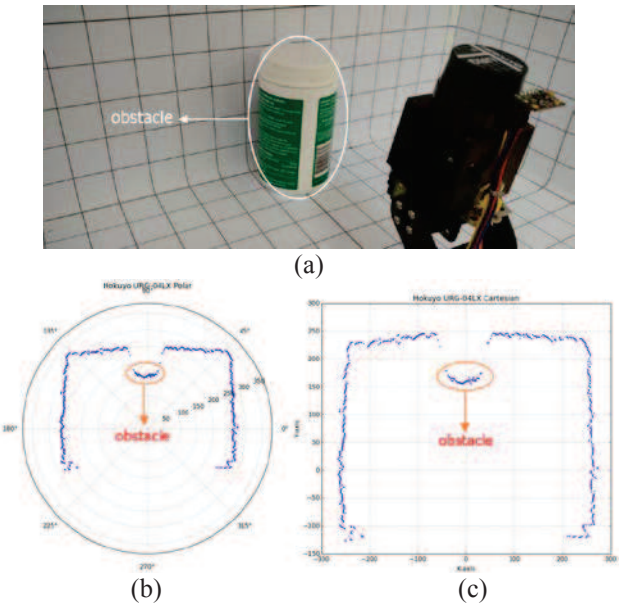

(a) (b) (c)

Fig. 8. (a) Obstacle pose (b) Polar plot (c) Cartesian plot

5.2 Output Smoothing of LRF Sensor

Noises at the output of LRF sensor are difficult to avoid and it is strongly influenced by the surfaces characteristic from the observed object, such as color and reflectivity of the light [11][12]. So it requires process of smoothing for the output of the LRF sensor. Gaussian filter is used in this work. Equation 13 shows the mathematical functions from the 1D gaussian filter. Figure 9 shows the results of filtering using 1D gaussian filter for the value of σ = 3 and 7.

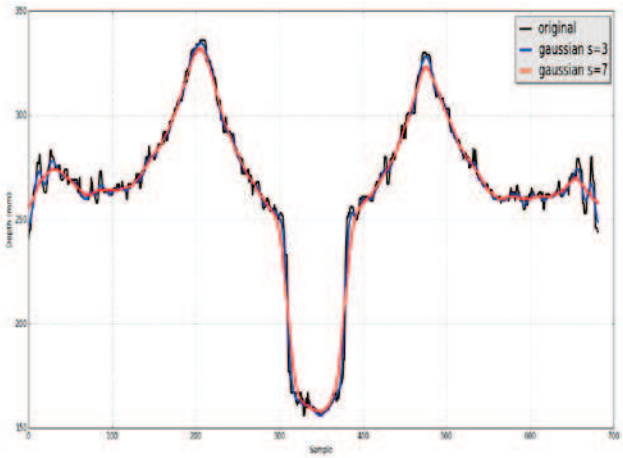

Fig. 9. 1D gaussian smoothing filter comparison

Based on the figure 9, with the value of sigma = 7 has provided a better filter output when compared with the value of sigma = 3. This is indicated by the number of ripples that occur throughout the measurement data.

5.3 Construct 3D Image

After filtering the output of the LRF sensor using 1D gaussian filter, the next step is building a 3D image based on the equation 5,6,7 from the several point of the angle of inclination (φ) which is read by the IMU sensor. Figure 10 shows the 3D image which successfully constructed.

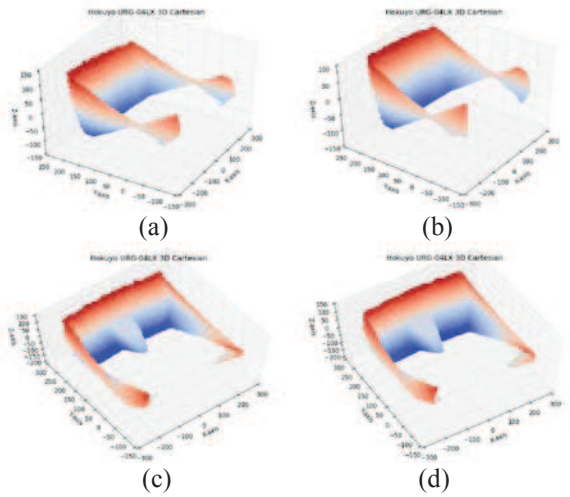

(a) (b) (c) (d)

Fig. 10. 3D image build (a) No obstacle – prior filtering (b) No obstacle – post filtering (c) With obstacle – prior filtering (d) With obstacle – post filtering

6. Conclusions

This paper presents a method of 3D image acquisition using 2D LRF sensor Hokuyo URG-04LX sensor with tilt servo mechanism which obtain correction tilt angle from the IMU sensor MPU6050. Filtering process was carried out to eliminate noise (smoothing), both from outputs of the IMU sensors and LRF sensor. Complementary filter does not much discussed in this paper and specifically discussed in another paper. In this work, LRF sensor output smoothed using a 1D gaussian filter. Based on the results of trials in 1D gaussian filter, better results are obtained with a value of $\sigma = 7$. Further research, developed a 3D SLAM with Kalman prediction to produce a better 3D map, and develop an object segmentation method which is used in the robot path planning.

References

[1] D. F. Wolf, G. S. Sukhatme, and S. Member, "Semantic Mapping Using Mobile Robots," *IEEE Trans. Robot.*, vol. 24, no. 2, pp. 245–258, 2008.

[2] C. Chen and Y. Cheng, "Research on Map Building by Mobile Robots," *IEEE - Second Int. Symp. Intell. Inf. Technol. Appl.*, pp. 673–677, Dec. 2008.

[3] B. B. Cortes, U. Valle, B. Piv, and X. C. Solé, "Indoor SLAM using a Range-Augmented Omnidirectional Vision," in *IEEE International Conference on Computer Vision Workshops*, 2011, pp. 280–287.

[4] M. Bosse, R. Zlot, and P. Flick, "Zebedee : Design of a Spring-Mounted 3-D Range Sensor with Application to Mobile Mapping," *IEEE Trans. Robot.*, vol. 28, no. 5, pp. 1104–1119, 2012.

[5] S. Oßwald and A. Hornung, "Autonomous Climbing of Spiral Staircases with Humanoids," *IEEE/RSJ Int. Conf. Intell. Robot. Syst. Sept. 25-30. San Fr. CA, USA*, pp. 4844–4849, 2011.

[6] Y.-S. Hawng, K. Hyun-Woo, and J.-M. Lee, "A 3D Map building algorithm using a single LRF on a mobile robot," in *9th International Conference on Ubiquitous Robots and Ambient Intelligence (URAI), November 25-29, Daejeon, Korea*, 2012, vol. 1, pp. 321–324.

[7] D. Magree and E. N. Johnson, "Combined Laser and Vision-aided Inertial Navigation for an Indoor Unmanned Aerial Vehicle," in *American Control Conference (ACC) June 4-6. Portland, Oregon, USA*, 2014, pp. 1900–1905.

[8] H. Kawata, A. Ohya, S. Yuta, W. Santosh, and T. Mori, "Development of ultra-small lightweight optical range," in *IEEE International Conference on Intelligent Robots and Systems (IROS)*, 2005, no. 42 50, pp. 1078 – 1083.

[9] InvenSense, "MPU-6000 and MPU-6050 Product Specification Rev 3.4," 2013.

[10] M. Ogaz, R. Sandoval, and M. Chacon, "Data Processing from a Laser Range Finder Sensor for the Construction of Geometric Maps of an Indoor Environment," in *Midwest Symposium on Circuits and Systems*, 2009, pp. 306–313.

[11] L. Kneip, F. Tache, G. Caprari, and R. Siegwart, "Characterization of the compact Hokuyo URG-04LX 2D laser range scanner," in *IEEE International Conference on Robotics and Automation*, 2009, pp. 1447–1454.

[12] Y. Okubo, C. Ye, and J. Borenstein, "Characterization of the Hokuyo URG-04LX Laser Rangefinder for Mobile Robot Obstacle Negotiation," 2009, vol. 7332, pp. 1–10.